$Ni/Ce_{0.8}Zr_{0.2}O_{2-x}$ Solid Solution Catalyst: A Pathway to Coke-Resistant CO_2 Reforming of Methane

Rubina Khatun[a], Rohan Singh Pal[a], Kapil Bhati[a], Anil Chandra Kothari[a,b], Shivani Singh[a], Nazia Siddiqui, Swati Rana[a,], Rajaram Bal[*a,b]

[a] Light Stock Processing Division, CSIR-Indian Institute of Petroleum, Dehradun 248005, India.

[b] Academy of Scientific and Innovative Research, Ghaziabad, Uttar Pradesh- 201002, India.

*Corresponding author: raja@iip.res.in; Fax: +91 135 2660202; Tel: +91 135 2525917

S1 Experimental:

S1.1 Materials

Nickel nitrate hexahydrate [$Ni(NO_3)_2.6H_2O$], cerium nitrate hexahydrate [$Ce(NO_3)_3.6H_2O$], zirconium oxynitrate hydrate [$ZrO(NO_3)_2.xH_2O$], citric acid anhydrous [$C_6H_8O_7$] (CA), were purchased from Sigma Aldrich. All the chemicals were of analytical grade and used as received without further purification for synthesis. Double distilled water was used in the preparation of all the aqueous solutions. Methane and carbon dioxide gases utilized in this study were purchased from Sigma gas services (New Delhi). The purity of all gases was higher than 99%.

S2.1 Catalyst preparation

The Ni/ZrO_2, Ni/CeO_2, and Ni/CeO_2-ZrO_2 catalysts were synthesized using a straightforward one-pot complex combustion method. The metal nitrate precursors were used for all the catalysts preparation. For a standard preparation of 5 wt.% $Ni/Ce_{0.8}Zr_{0.2}O_{2-x}$ catalyst, the 2.01 g of $Ce(NO_3)_2.6H_2O$, 0.37 g of $ZrO(NO_3)_2.xH_2O$ and 0.24 g of $Ni(NO_3)_2.6H_2O$ were dissolved in 40 mL double-distilled water in 250 mL beaker. Meanwhile, the aqueous solution of 1.35 g of citric acid was prepared into 10 mL double distilled water. The molar ratio of citric acid and metal precursors was maintained to unity. After getting a clear solution, a dropwise slow addition of aqueous citric acid was carried out under continuous stirring at room temperature for complexation. After 1 h stirring at room temperature, the resultant solution was heated at 80 °C on a hot plate. Once the material turns into spongy gel, the temperature of hot plate quickly raised to 150 °C for combustion process. The combustion of a spongy semi-solid

occurred shortly after, with an increase in temperature and gas evolution, due to the exothermic reaction between metal precursors and citric acid. The resultant powder was cooled down naturally to ambient temperature and crushed into a fine powder for calcination. The calcination process was conducted in ambient air at 750 °C for 4 h. The final catalyst has been named as 5NCZ. Additionally, catalysts containing 5 wt.% Ni/ZrO_2 and Ni/CeO_2 were synthesized using the appropriate amounts of their respective precursors according to the previously described method. These were designated as 5NZ and 5NC, respectively. We also prepared 2.5 and 7.5 wt.% $Ni/Ce_{0.8}Zr_{0.2}O_{2-x}$ catalysts to optimize the nickel loading for DRM and designated as 2.5NCZ and 7.5NCZ, respectively.

S1.3 Catalytic characterization:

The crystal structure and phase purity were confirmed by powder X-ray diffraction (XRD) on a Proto Advance X-ray diffractometer fitted with a Lynx eye high-speed strip detector in the 2θ range 10-80° using Cu Kα (λ = 0.154 nm) as an incident beam.

Surface area analysis was done by Micromeritics ASAP 2020 Surface Area and Porosity Analyser using the BET equation at -196 °C. Before each experiment, the catalyst was degassed at 240 °C for 3 h under vacuum.

Thermogravimetric analysis (TGA/DTG) of the samples was carried out by Thermogravimetric analyzer TGA 8000 (Perkin Elmer) instrument using oxygen in the temperature range of 30-900 °C.

The transmission electron microscopy (TEM) analysis was performed using a JEM-2100 system (JEOL, Japan), operated at an accelerating voltage of 200 kV. The instrument is equipped with a LaB_6 (lanthanum hexaboride) electron source. Selected Area Electron Diffraction (SAED) patterns were obtained to analyze the crystalline structure of the samples. The TEM is also equipped with an energy-dispersive X-ray spectroscopy (EDS) detector for elemental analysis and mapping. For TEM analysis, all the samples were prepared by dispersing materials in ethanol mounted on a lacey carbon formvar Cu grid.

Inductive coupled plasma atomic emission spectroscopic (ICP-AES) was performed using PS 3000 UV, Leeman Labs Inc, (USA) to check the composition of the metals (wt.%) in the catalyst system.

Temperature programmed reduction (TPR) and H_2 chemisorption experiments were carried out in a Micromeritics, Auto-Chem II 2920 instrument connected with a thermal conductivity

detector (TCD). Initially, 0.05 g sample was first pretreated under a He stream at 873 K for 120 min, and then cooled to room temperature. A 10% H_2/Ar stream (20 mL/min) was passed over the sample while it was being heated from room temperature to 1173 K at a heating rate of 10 K/min.

To find the oxidation state of the catalysts, an X-ray photoelectron spectroscopy (XPS) analysis was performed. X-ray photoelectron spectra were recorded on a Thermo Scientific K-alpha X-ray photoelectron spectrometer, and binding energies (± 0.2 eV) were determined with respect to the position of the C 1s peak at 284.6 eV.

The Raman spectra of the catalysts were measured using a laser with a wavelength of 532 nm on a HORIBA Scientific LabRAM HR Evolution Raman spectrometer with an argon laser excitation source. The range of scanned Raman shifts is 50 to 2000 cm^{-1}.

Inductively Coupled Plasma Atomic Emission Spectroscopic (ICP-AES) analysis was carried out by Inductively Coupled Plasma Atomic Emission Spectrometer; model: PS 3000 UV, (DRE), Leeman Labs, Inc, (USA).

O_2-TPD was carried out in a Micromeritics, Auto-Chem II 2920 instrument connected with a thermal conductivity detector (TCD). Firstly, the sample (60 mg) was heated from room temperature to 200 °C in a He flow of 30 mL/min, which was maintained for 100 min, before the sample was cooled to room temperature (still in an He atmosphere), and then the sample was exposed to a stream of pure O_2 (10 mL/min) for 30 min. The sample was then exposed to a He flow for 30 min to clear residual oxygen. After that, it was heated from room temperature to 700 °C in He atmosphere at 10 °C/min. The O_2 consumption was continuously analysed using TCD.

The CO_2-TPD reaction was performed with a Micromeritics, Auto Chem II 2920 (Micromeritics, GA, USA) instrument connected to a thermal conductivity detector (TCD) to check the basicity of the as synthesized catalysts. In order to do this, a 50 mg catalyst was used for the test in a 30 mL/min He flow. To prevent any possible impurities, the sample was heated to 400 °C and held for 30 minutes prior to the test. The sample was then cooled to 50 °C, and then the sample was subjected to a 40 mL/min 10% CO_2 balance He flow for 90 min to completely saturate the surface, followed by a 30 mL/min ultra-high purity He flow for 30 minutes to remove any physically adsorbed CO_2. After all of these pre-treatments, the catalyst was heated at a rate of 10 °C/min from 50 to 800 °C to collect desorption data using TCD.

S1.3 Reaction setup and activity measurement

Typically, in a quartz reactor tube having an internal diameter of 6 mm and a length of 35 cm, 80 mg catalyst placed in between two quartz wool plugs in the center of this tube. Before the reaction, the catalyst was reduced at 500 °C for 2 h with the flow of 20% H_2 balanced N_2 (35 mL/min). After reduction, the catalyst was cooled down to reaction temperature and feed gases were introduced into the reactor. Brooks mass flow controllers were used to control the flow rates of the gases. Catalytic performance was investigated in the temperature range of 400-800 °C with a molar ratio of CH_4: CO_2: N_2 =1:1:8. Time-on-stream study of the catalysts was performed at 700 °C temperature where GHSV was 50,000 $mLg^{-1}h^{-1}$. The reaction products were analyzed by using an online refinery gas analyzer (Agilent 7890B) fitted with one FID and two TCD detectors. HP-plot-Q column was used for the detection of CH_4 in FID and molecular sieve, hayesep Q, and porapack Q columns were used for the detection of H_2, CO, and CO_2 in TCD. A detailed carbon balance was performed for each experiment, and the result was between 97 and 102%.

S2. Results and discussion

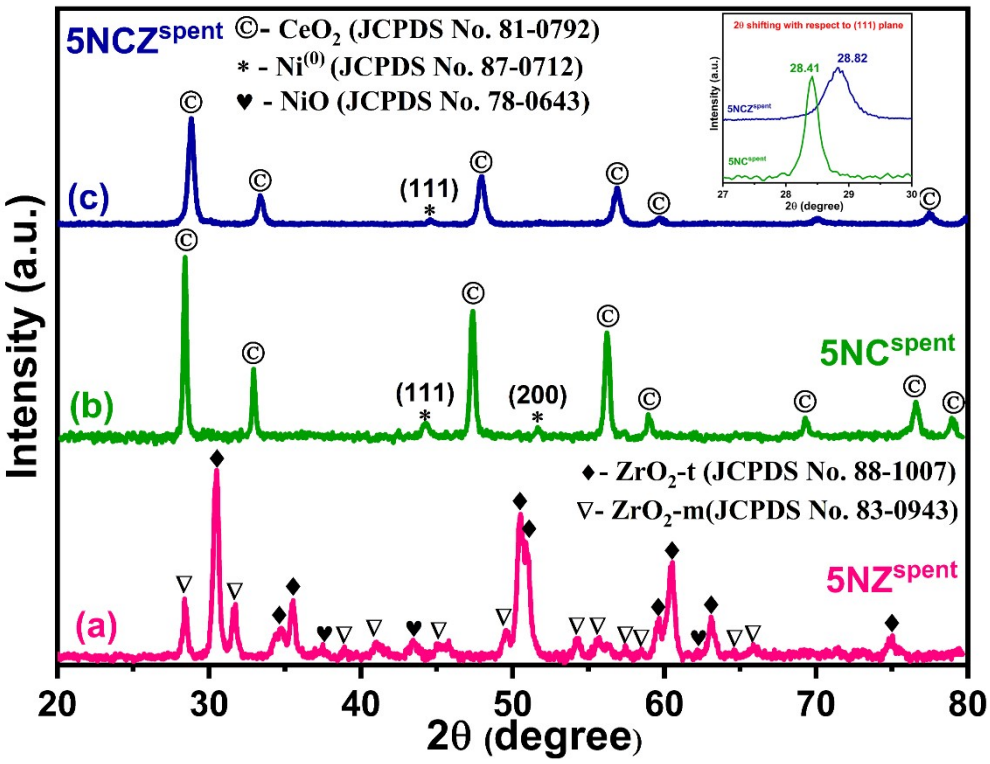

Fig. S1 XRD patterns of $5NZ^{spent}$ (a), $5NC^{spent}$ (b) and $5NCZ^{spent}$ (c) catalysts

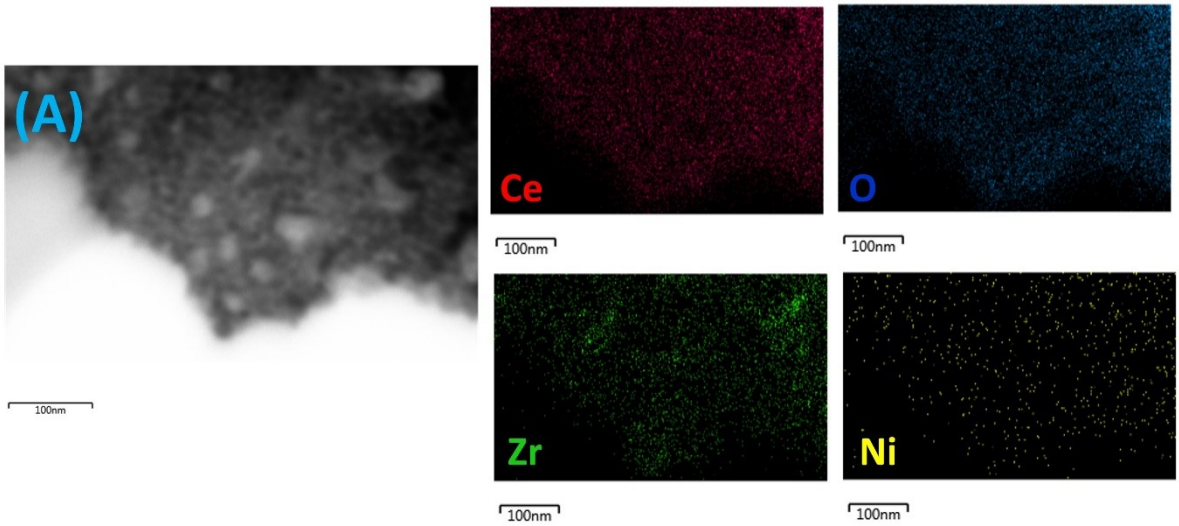

Fig. S2 Elemental mapping and respective image of freshly reduced 5NCZ catalyst

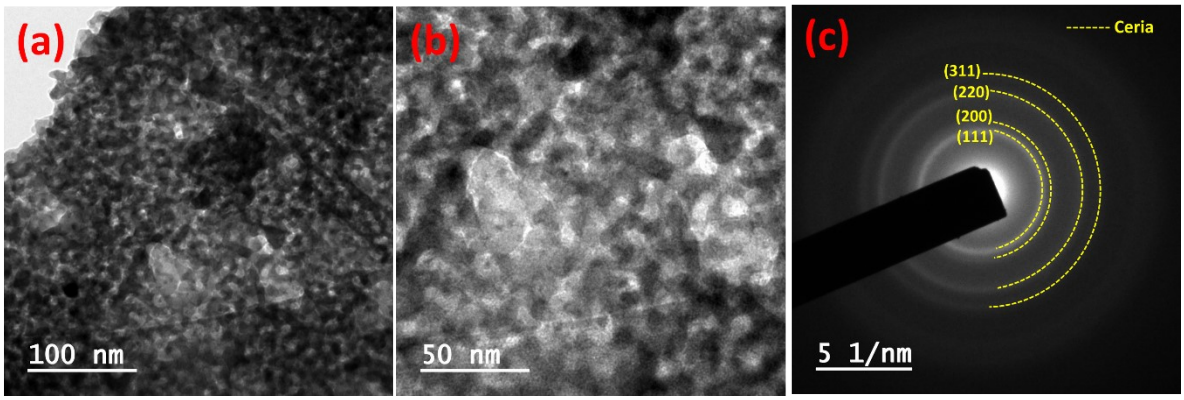

Fig. S3 TEM images (a and b) and SAED pattern (c) of spent 5NCZ catalyst

Table S1: H_2 consumption (µmol/g) by all the fresh catalyst

Catalyst	H_2 consumption for NiO and active oxygen species (100-500 °C)	H_2 consumption for bulk oxygen (500-900 °C)	Total H_2 consumption
5NZ	54.4	-	54.4
5NC	80.3	53.5	133.8
5NCZ	107.1	41.5	148.6

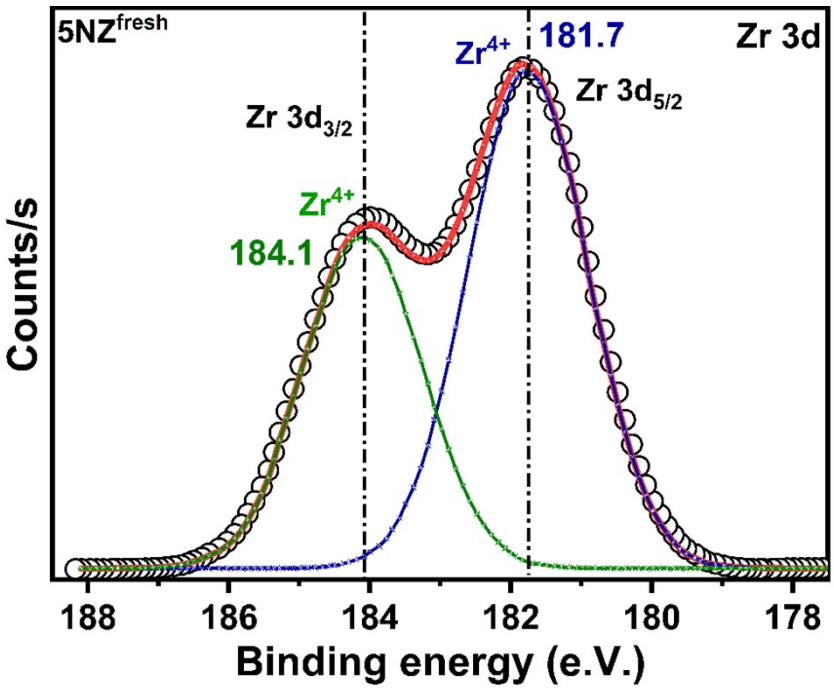

Fig. S4 Zr 3d XPS spectra of fresh 5NZ catalyst

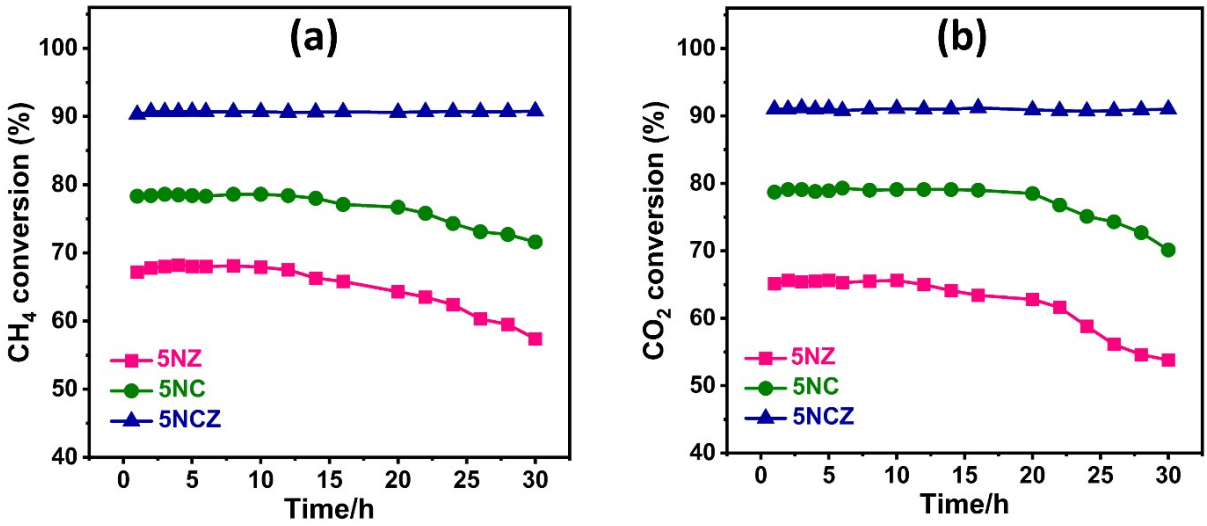

Fig. S5 TOS (30 h) test over the 5NZ, 5NC and 5NCZ catalyst. (a) CH_4 conversion and (b) CO_2 conversion (Reaction condition: Temperature- 700 °C, Pressure-1 atm, GHSV- 50, 000 $mLg^{-1}h^{-1}$, feed ratio CH_4:CO_2:N_2-1:1:8)

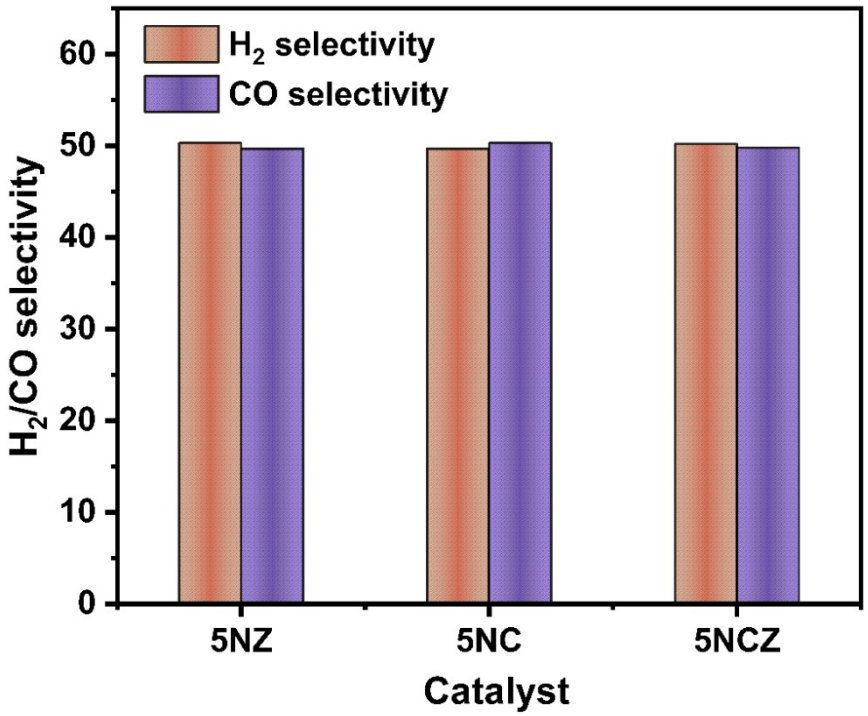

Fig. S6 Represent the H_2 and CO selectivity of 5NZ, 5NC and 5NCZ catalyst at 700 ºC (Reaction condition: Pressure – 1 atm, feed ratio- CH_4:CO_2:N_2 – 1:1:8, GHSV- 50,000 $mLh^{-1}g^{-1}$)

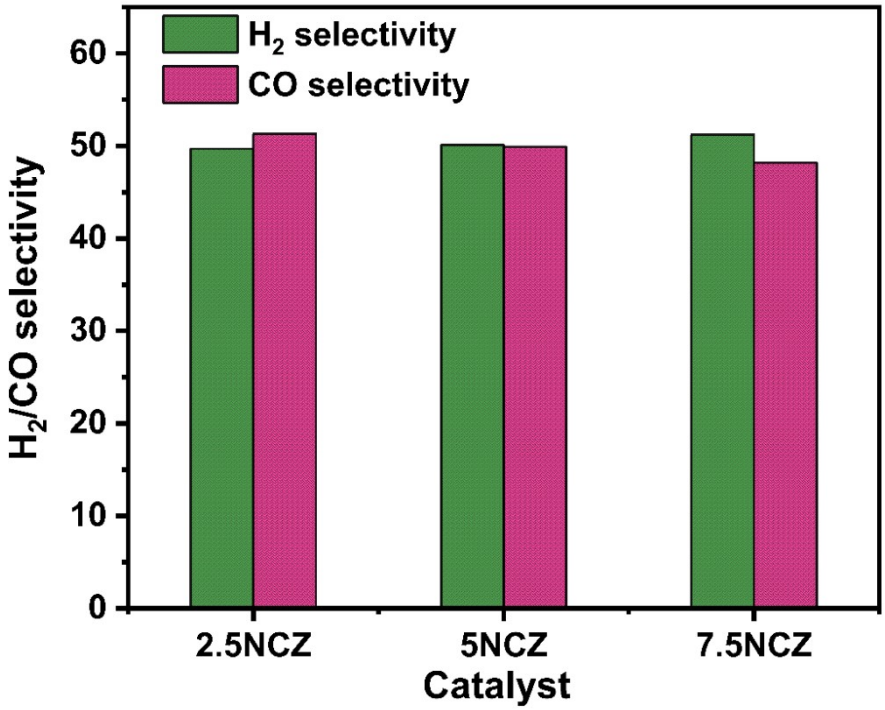

Fig. S7 Represent the H_2 and CO selectivity of 2.5NCZ, 5NCZ and 7.5NCZ catalyst at 700 ºC (Reaction condition: Pressure – 1 atm, feed ratio- CH_4:CO_2:N_2 – 1:1:8, GHSV- 50,000 $mLh^{-1}g^{-1}$)

Comparative analysis of catalyst performance for DRM reaction: To provide a clearer perspective, we have included a comparative analysis of our catalyst performance (e.g., CH_4 and CO_2 conversion, H_2/CO ratio and stability) with those of other Ni-based catalysts reported in the literature (shown below).

Table S2: Comparative analysis of catalyst performance for DRM reaction

Catalyst	Temp. (ºC)	CH_4 Conversion (%)	CO_2 Conversion (%)	H_2/CO ratio	Stability (h)	Ref.
Ni/CeO_2-Al_2O_3	800	73-74	82-84	0.70 - 0.85	72	*1*
Ni-Cu/CeO_2	800	80	85	0.96	20	*2*
Ni/MgO	700	94	79	0.8 - 0.85	24	*3*
Ni/SBA-15	700	> 70	> 70	~ 1.0	100	*4*
Ni/MCM-41	700	> 40	> 40	~ 0.75	7	*5*
Ni/ZrO_2	700	~ 50	~ 50	~ 1.0	5	*6*
Mg(Ni)Al_2O_4	850	> 85	> 85	1.2 - 1.4	200	*7*
Ni-Co/Al_2O_4	750	> 80	> 80	0.7	10	*8*
Ni/$MgAl_2O_4$	750	> 80	> 80	0.99	55	*9*
Ni/La_2O_3	700	70	75	0.87	50	*10*
Ni-MgO/Al_2O_3	800	> 40	> 40	0.7	50	*11*
NiSc/Al_2O_3	800	93.2	> 98	~ 1.0	30	*12*
Ni/MgO-SBA-15	700	≥ 55	≥ 55	0.9	40	*13*
Ni@SiO_2@CeO_2	600	68	80	0.8	30	*14*
Ni/CeO_2/Al_2O_3	800	75	85	0.9	25	*15*
Ni/MCM-41	700	75	86	1.03	10	*16*
Ni@MA	750	77.8	87.5	1.25	4	*17*
NiB(x)/y-Al_2O_3	700	91.3	66.3	1	24	*18*
Ni/Ce-Sm-Cu-O	750	76	76	0.9	12	*19*
Ni-Co/CeO_2-$ZnAl_2O_4$	700	76	74	0.99	8.5	*20*
Ni/$Ce_{0.8}Zr_{0.2}O_{2-x}$	***700***	***90.8***	***91***	***1.0***	***100***	***This work***

Reaction set-up: The schematic presentation of the reaction set-up for dry reforming of methane is shown below (Fig. S8).

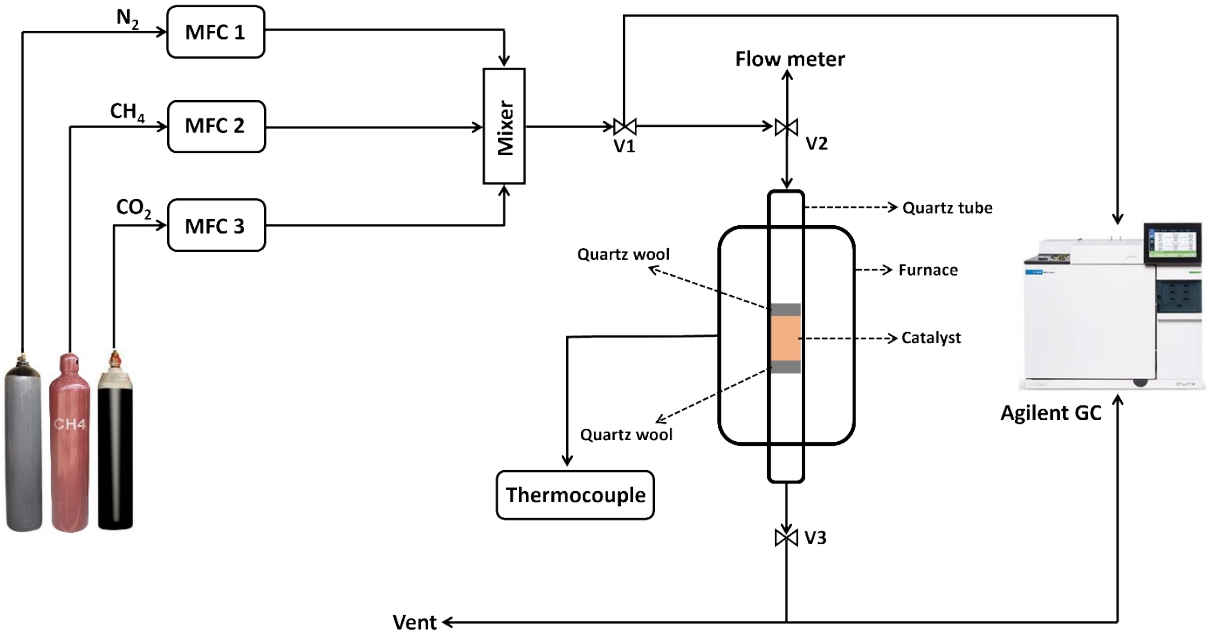

Fig. S8 Schematic presentation of the reaction set-up for dry reforming of methane

References:

(1) Marinho, A. L.; Toniolo, F. S.; Noronha, F. B.; Epron, F.; Duprez, D.; Bion, N. Highly active and stable Ni dispersed on mesoporous CeO2-Al2O3 catalysts for production of syngas by dry reforming of methane. *Applied Catalysis B: Environmental* **2021**, *281*, 119459.

(2) Sagar, T.; Padmakar, D.; Lingaiah, N.; Sai Prasad, P. Influence of solid solution formation on the activity of CeO 2 supported Ni–Cu mixed oxide catalysts in dry reforming of methane. *Catalysis Letters* **2019**, *149*, 2597-2606.

(3) Danghyan, V.; Kumar, A.; Mukasyan, A.; Wolf, E. An active and stable NiOMgO solid solution based catalysts prepared by paper assisted combustion synthesis for the dry reforming of methane. *Applied Catalysis B: Environmental* **2020**, *273*, 119056.

(4) Zhang, Q.; Zhang, T.; Shi, Y.; Zhao, B.; Wang, M.; Liu, Q.; Wang, J.; Long, K.; Duan, Y.; Ning, P. A sintering and carbon-resistant Ni-SBA-15 catalyst prepared by solid-state grinding method for dry reforming of methane. *Journal of CO2 Utilization* **2017**, *17*, 10-19.

(5) Fakeeha, A. H.; Kasim, S. O.; Ibrahim, A. A.; Abasaeed, A. E.; Al-Fatesh, A. S. Influence of nature support on methane and CO2 conversion in a dry reforming reaction over nickel-supported catalysts. *Materials* **2019**, *12* (11), 1777.

(6) Zhang, M.; Zhang, J.; Wu, Y.; Pan, J.; Zhang, Q.; Tan, Y.; Han, Y. Insight into the effects of the oxygen species over Ni/ZrO2 catalyst surface on methane reforming with carbon dioxide. *Applied Catalysis B: Environmental* **2019**, *244*, 427-437.

(7) Abbas, M.; Sikander, U.; Mehran, M. T.; Kim, S. H. Exceptional stability of hydrotalcite derived spinel Mg (Ni) Al2O4 catalyst for dry reforming of methane. *Catalysis Today* **2022**, *403*, 74-85.

(8) Aghaali, M. H.; Firoozi, S. Enhancing the catalytic performance of Co substituted NiAl2O4 spinel by ultrasonic spray pyrolysis method for steam and dry reforming of methane. *International Journal of Hydrogen Energy* **2021**, *46* (1), 357-373.
(9) Guo, J.; Lou, H.; Zhao, H.; Chai, D.; Zheng, X. Dry reforming of methane over nickel catalysts supported on magnesium aluminate spinels. *Applied Catalysis A: General* **2004**, *273* (1-2), 75-82.
(10) Li, X.; Li, D.; Tian, H.; Zeng, L.; Zhao, Z.-J.; Gong, J. Dry reforming of methane over Ni/La2O3 nanorod catalysts with stabilized Ni nanoparticles. *Applied Catalysis B: Environmental* **2017**, *202*, 683-694.
(11) Jin, B.; Li, S.; Liang, X. Enhanced Activity and Stability of MgO-Promoted Ni/Al_2O_3 Catalyst for Dry Reforming of Methane: Role of MgO. **2021**.
(12) Zhao, X.; Cao, Y.; Li, H.; Zhang, J.; Shi, L.; Zhang, D. Sc promoted and aerogel confined Ni catalysts for coking-resistant dry reforming of methane. *RSC advances* **2017**, *7* (8), 4735-4745.
(13) Wang, N.; Yu, X.; Shen, K.; Chu, W.; Qian, W. Synthesis, characterization and catalytic performance of MgO-coated Ni/SBA-15 catalysts for methane dry reforming to syngas and hydrogen. *International journal of hydrogen energy* **2013**, *38* (23), 9718-9731.
(14) Han, K.; Yu, W.; Xu, L.; Deng, Z.; Yu, H.; Wang, F. Reducing carbon deposition and enhancing reaction stability by ceria for methane dry reforming over Ni@ SiO2@ CeO2 catalyst. *Fuel* **2021**, *291*, 120182.
(15) Luisetto, I.; Tuti, S.; Battocchio, C.; Mastro, S. L.; Sodo, A. Ni/CeO2–Al2O3 catalysts for the dry reforming of methane: the effect of CeAlO3 content and nickel crystallite size on catalytic activity and coke resistance. *Applied Catalysis A: General* **2015**, *500*, 12-22.
(16) Frontera, P.; Macario, A.; Aloise, A.; Antonucci, P.; Giordano, G.; Nagy, J. Effect of support surface on methane dry-reforming catalyst preparation. *Catalysis today* **2013**, *218*, 18-29.
(17) Arbag, H. Effect of impregnation sequence of Mg on performance of mesoporous alumina supported Ni catalyst in dry reforming of methane. *International Journal of Hydrogen Energy* **2018**, *43* (13), 6561-6574.
(18) Fouskas, A.; Kollia, M.; Kambolis, A.; Papadopoulou, C.; Matralis, H. Boron-modified Ni/Al2O3 catalysts for reduced carbon deposition during dry reforming of methane. *Applied Catalysis A: General* **2014**, *474*, 125-134.
(19) Hussien, A. G.; Damaskinos, C. M.; Dabbawala, A. A.; Anjum, D. H.; Vasiliades, M. A.; Khaleel, M. T.; Wehbe, N.; Efstathiou, A. M.; Polychronopoulou, K. Elucidating the role of La3+/Sm3+ in the carbon paths of dry reforming of methane over Ni/Ce-La (Sm)-Cu-O using transient kinetics and isotopic techniques. *Applied Catalysis B: Environmental* **2022**, *304*, 121015.
(20) Movasati, A.; Alavi, S. M.; Mazloom, G. Dry reforming of methane over CeO2-ZnAl2O4 supported Ni and Ni-Co nano-catalysts. *Fuel* **2019**, *236*, 1254-1262.